

## COMMUNICATION

[View Article Online](#)  
[View Journal](#) | [View Issue](#)



Cite this: *Dalton Trans.*, 2025, **54**, 12125

Received 13th June 2025,  
Accepted 16th July 2025

DOI: 10.1039/d5dt01395j

rsc.li/dalton

## A detailed study on the effects of adsorbed water molecules on proton conduction in a metal–organic framework<sup>†</sup>

Kyoko Shiraishi,<sup>a</sup> Mitsuki Kabaya,<sup>a</sup> Kouki Fujihira,<sup>a</sup> Kenichi Kato<sup>b</sup> and Masaaki Sadakiyo  <sup>\*a</sup>

We demonstrate the proton-conductive properties of Zr-BPT, having one-dimensional pores. The MOF shows superprotic conductivity of  $3.6 \times 10^{-4}$  S cm<sup>-1</sup> at room temperature (25 °C). The conduction mechanism was discussed with the relationship among the structure, conductive properties, and adsorption behaviour.

Due to the importance of fuel cell technology, proton conductors have garnered considerable attention over the past several decades.<sup>1</sup> Recently, metal–organic frameworks (MOFs) have become an important class of proton conductors because of their excellent ability for accepting guest molecules that enhance proton conductivity through constructing efficient proton-conducting pathways inside the channels.<sup>2</sup> The most studied and well-known guest molecule for enhancing proton conductivity is the water molecule (H<sub>2</sub>O),<sup>3</sup> while some other guests, such as imidazole, have also been studied.<sup>4</sup>

The characteristic feature of proton conduction mediated by water molecules is the presence of two distinct conduction mechanisms, vehicle mechanism<sup>5</sup> and Grotthuss mechanism,<sup>6</sup> the former is the direct diffusion of the protonated species (e.g., H<sub>3</sub>O<sup>+</sup>) and the latter is the more efficient way in which protons transfer like a baton relay through hydrogen bonds with adjacent atoms (more precisely described as the generation of H<sub>5</sub>O<sub>2</sub><sup>+</sup> and H<sub>9</sub>O<sub>4</sub><sup>+</sup>).<sup>7</sup> So far, numerous studies on water-mediated proton-conducting MOFs have been reported, and many researchers have attempted to elucidate the relationship between the MOF structure (*i.e.*, ion-conducting pathway) and its ion-conductive properties. For instance, some research studies revealed the dependence of proton conductivity on water vapor pressure (*i.e.*, humidity) by employing MOFs with

well-defined structures.<sup>8,9</sup> There is a clear consensus that the presence of certain structural features enabling the Grotthuss mechanism is critical for achieving high proton conductivity at ambient temperature.<sup>2,3,7,10</sup> Regarding this point, many papers predict the existence of the Grotthuss mechanism based on the activation energy (E<sub>a</sub>) values: when the activation energy is lower than 0.4 eV, the mechanism is determined to be Grotthuss.<sup>10</sup> However, as far as we know, this is an ambiguous criterion, and we could not find any definitive experimental studies on this point, although the tendency for the Grotthuss mechanism to exhibit low activation energy due to the low energy requirement (~0.11 eV) of hydrogen-bond cleavage has been theoretically suggested.<sup>6,10</sup> Since MOFs have well-defined structures and a precise number of adsorbed water molecules (depending on the partial pressure) with a wide range of adsorption amounts, this aspect could be clearly elucidated.

In this study, we demonstrated a clear relationship among the number of adsorbed water molecules, ionic conductivity, and activation energy by employing a water-stable Zr-based MOF, Zr-BPT (Zr<sub>12</sub>O<sub>8</sub>(OH)<sub>8</sub>(HCOO)<sub>15</sub>(BPT)<sub>3</sub>) (H<sub>3</sub>BPT = [1,1'-biphenyl]-3,4',5-tricarboxylic acid), having well-defined small (~5.6 Å) one-dimensional (1-D) channels constructed from typical Zr<sub>6</sub> clusters connected by BPT<sup>3-</sup> ligands (Fig. 1).<sup>11</sup> Zr-BPT showed superprotic conductivity of  $3.6 \times 10^{-4}$  S cm<sup>-1</sup> under 0.98 P/P<sub>0</sub> (*i.e.*, 98% relative humidity (RH)) at room temperature (25 °C). It also showed a large amount of water vapor adsorption, depending on the partial pressure (P/P<sub>0</sub>), and thus exhibited strong dependence of proton conductivity on the partial pressure of water vapor (in the range from 10<sup>-12</sup> to 10<sup>-4</sup> S cm<sup>-1</sup>). The relationship between the number of adsorbed water molecules and ionic conductivity clearly indicated that the drastic increase in proton conductivity occurred by adsorbing more than approximately 30 water molecules because of the presence of the Grotthuss mechanism, which is also predicted by theoretical simulations. The plot of activation energy depending on the number of adsorbed water molecules clearly indicates that there is a clear change in the activation energy depending on the conducting mechanism,

<sup>a</sup>Department of Applied Chemistry, Faculty of Science Division I, Tokyo University of Science, 1-3 Kagurazaka, Shinjuku-ku, Tokyo 162-8601, Japan.

E-mail: [sadakiyo@rs.tus.ac.jp](mailto:sadakiyo@rs.tus.ac.jp)

<sup>b</sup>RIKEN Spring-8 Center, 1-1-1 Kouto, Sayo-cho, Sayo-gun, Hyogo 679-5148, Japan

† Electronic supplementary information (ESI) available: Details of synthesis and physical measurements; Nyquist plots; XRPD patterns; modelled structures of adsorbed water molecules; and temperature dependence of proton conductivity.

See DOI: <https://doi.org/10.1039/d5dt01395j>



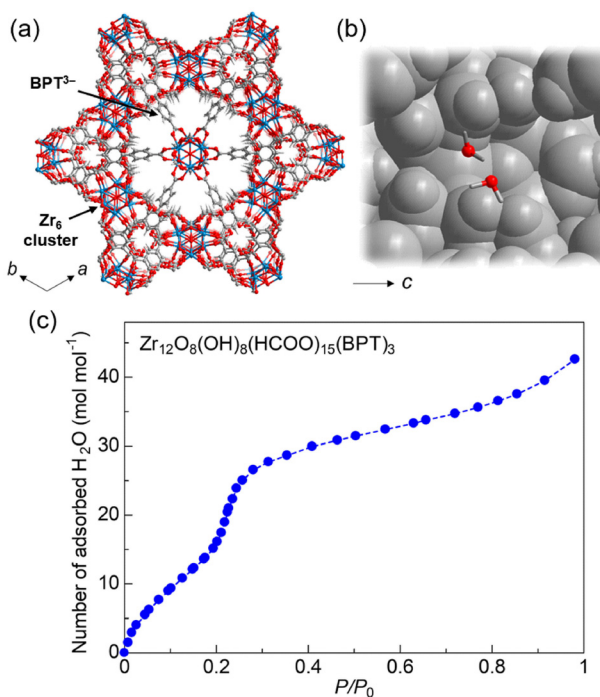


**Fig. 1** (a) Representation of the structure of porous Zr-BPT along the  $c$ -axis. (b) Representation of a modelled structure of adsorbed water molecules in the 1-D channel by Monte Carlo searches (with 5 water molecules per formula unit). (c) Water vapor adsorption isotherms of Zr-BPT at 25 °C.

and we found that the activation energy of 0.4 eV is an ambiguous indicator for determining the conduction mechanism in proton-conducting MOFs.

The sample, Zr-BPT, was prepared according to the previous literature.<sup>11</sup> Prior to evaluating the proton conductivity of Zr-BPT, the adsorption behaviour for water molecules was evaluated by water vapor adsorption isotherm measurements. As shown in Fig. 1c, Zr-BPT shows a large amount of adsorption of water molecules, depending on the partial pressure of water vapor. The adsorption amount was continuously increased below 0.2  $P/P_0$  and was increased more gradually above 0.3  $P/P_0$ . At maximum, Zr-BPT adsorbs more than 40 molecules per formula unit at high partial pressure. As shown in Fig. 1b, the result of Monte Carlo simulation (discussed later) clearly indicates that Zr-BPT has an ability to adsorb water molecules in the channels even if its size is very small, and is consistent with this experimental result. Compared with the water vapor adsorption isotherms of hydrophobic<sup>12</sup> or hydrophilic MOFs,<sup>13</sup> we could state that the hydrophilicity (or hydrophobicity) of the pores of Zr-BPT is moderate. Zr-BPT exhibits a wide range of adsorption capacities over a broad pressure region, which is experimentally advantageous for elucidating the relationship between proton conductivity and adsorption amount. Note that we previously reported the excellent stability of this MOF for water, even in basic ( $\text{pH} < 12$ ) or acidic ( $\text{pH} > 0$ ) solutions,<sup>11</sup> which is also necessary to perform detailed evaluations about the proton-conductive properties.

The ionic conductivity of Zr-BPT was evaluated by alternating-current impedance measurements under water vapor with controlled partial pressure by employing a home-made sealed cell which was used for conductivity measurements under various guest vapors.<sup>14</sup> Fig. 2 shows the partial pressure dependence of ionic conductivity (Nyquist plots are shown in Fig. S1 and S2†). At high humidity, the MOF shows superionic conductivity of  $3.6 \times 10^{-4} \text{ cm}^{-1}$  ( $0.98 P/P_0$ ) at 25 °C. Considering the fact that Zr-BPT does not include any ionic carriers and that the conductivity drastically increased with the partial pressure of water vapor (*i.e.*, humidity), the ionic conductivity of Zr-BPT should be attributed to proton conduction caused by the adsorbed water molecules in its pores. This kind of high proton conductivity was often observed in various MOFs that adsorb a large amount of water molecules as guests.<sup>15</sup> In these cases, the ionic carriers, *i.e.*, protons, are provided by self-dissociation of water molecules, and they migrate in the pores with the help of water molecules as the conducting media. The full-range data (*i.e.*, from 0 to almost 1  $P/P_0$ ) of the partial pressure dependence of proton conductivity and the water vapor adsorption isotherms allowed us to disclose the relationship between ionic conductivity and the number of adsorbed guest (*i.e.*, water) molecules (Fig. 3). As shown in Fig. 3, the proton conductivity of Zr-BPT is not remarkably increased below 30 molecules and thus it shows a low conductivity of around  $10^{-10}$ – $10^{-8} \text{ S cm}^{-1}$  in this region. In contrast, above 30 molecules, the conductivity drastically increased with increasing number of water molecules and it finally reached superprotic conductivity above  $10^{-4} \text{ S cm}^{-1}$ .

To get information about the structure of Zr-BPT under various partial pressures, we performed *in situ* X-ray powder diffraction (XRPD) on the RIKEN Materials Science I Beamline BL44B2 located at SPring-8.<sup>16</sup> Almost the same patterns (Fig. S3†) observed under different humidity conditions ( $P/P_0 = 0, 0.1, 0.5, 0.7, 1$ ) confirmed that the framework structure of Zr-BPT was not changed during the adsorption process, while some significant increase in adsorption amount (*e.g.*, ~0.3

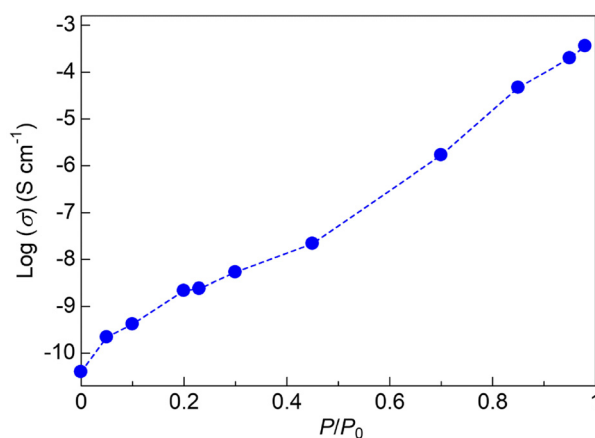


**Fig. 2** Dependence of proton conductivity of Zr-BPT (25 °C) on the partial pressure of water vapor.



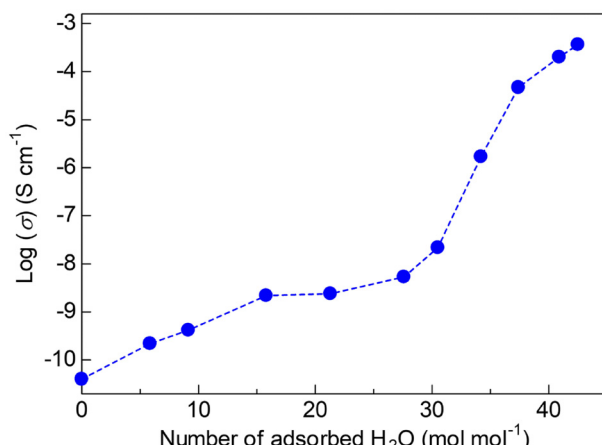


**Fig. 3** Relationship between proton conductivity (25 °C) and the number of adsorbed water molecules in Zr-BPT.

$P/P_0$ ) was observed in the adsorption isotherms (Fig. 1c). This result clearly indicates that the framework of Zr-BPT is robust and classified into a 2nd generation compound.<sup>17</sup> Some peaks were slightly shifted depending on the humidity (Fig. S3†), indicating the adsorption of water molecules inside the channels. Note that the determination of the exact position of water molecules in the MOF through Rietveld analysis failed because of its disordered character. On the other hand, we could extract important information about the arrangement of the adsorbed water molecules through the pore volume. The solvent-accessible pore volume of Zr-BPT was calculated to be 19.3%, *i.e.*, 1201 Å<sup>3</sup> per formula unit, using the PLATON software.<sup>18</sup> Since the average volume of a water molecule in bulk water is about 30 Å<sup>3</sup>,<sup>19</sup> the maximum capacity of the pores of Zr-BPT is expected to be around 40 molecules, which is consistent with the result of adsorption isotherms. Therefore, it is evident that the drastic increase in proton conductivity begins just before the channels become fully occupied by water molecules (>30 molecules). This clearly suggests that the Grotthuss mechanism becomes dominant above this region due to the sufficiently short distance between adjacent water molecules in the channels. To provide a more detailed picture of this point, we visualized the modelled structures of the adsorbed water molecules on different numbers of guests (20 and 40 molecules per formula unit), using Monte Carlo simulation through the Adsorption Locator equipped in the Materials Studio software (Fig. S4†).<sup>20</sup> In the case of a small adsorption amount (*i.e.*, 20 molecules), some considerably short distances (<3.2 Å) between neighbouring water molecules are observed, indicating the possibility of hydrogen bond formation. However, there are also instances of large separations between water molecules. This clearly indicates that the long-range transfer of generated proton carriers only through hydrogen-bonding networks, *i.e.*, the Grotthuss mechanism, is impossible, and that the vehicle mechanism must be included in the migration process of the proton carriers in this state. On the other hand, in the case of a large adsorption amount (*i.e.*,

40 molecules), large separations between water molecules are not observed; instead, they are closely arranged with short distances (<3.2 Å) in the channels. This clearly indicates that infinite hydrogen-bonding networks are possibly formed in the fully occupied state, enabling long-range proton transfer *via* the Grotthuss mechanism.

Since the temperature dependence of proton conductivity at each partial pressure was also evaluated (Fig. S5†), we succeeded in plotting the dependence of activation energy on the number of adsorbed water molecules in Zr-BPT (Fig. 4). In the region of low adsorption amount (approximately below 30 molecules), the activation energy is almost constant at around 0.3 eV. In contrast, in the region of larger adsorption amount, the activation energy decreases with increasing adsorption amount, finally reaching a very low activation energy of around 0.1 eV above 40 molecules (*i.e.*, “fully-occupied” region). According to the discussions described above, the clear tendency of decreasing activation energy in the region of large adsorption amounts is attributable to a change in the conduction mechanism; the Grotthuss mechanism becomes dominant due to the formation of hydrogen-bonding networks among closely packed water molecules. This is consistent with the previously predicted understanding.<sup>10</sup> However, the important point which we highlight in this study is that the commonly used criterion value of 0.4 eV for distinguishing the vehicle mechanism (>0.4 eV) from the Grotthuss mechanism (<0.4 eV) is somewhat ambiguous. Although there is literature describing the contribution of the vehicle mechanism even at activation energies below 0.4 eV,<sup>21</sup> we were unable to find any examples of proton-conducting MOFs that are structurally characterized as exhibiting the vehicle mechanism and also have an activation energy below 0.4 eV, independent of the empirical threshold. In almost all previous studies, the conduction mechanism has been determined primarily based on the activation energy value, without questioning the validity of this empirical criterion. Our results suggest that this point should be carefully considered when

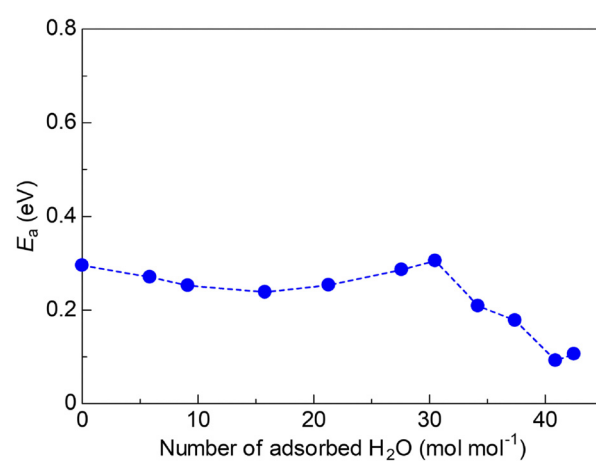


**Fig. 4** Relationship between the activation energy of the proton conduction in Zr-BPT and the number of adsorbed water molecules.

discussing the conduction mechanism of proton-conducting MOFs. To the best of our knowledge, this is the first experimental demonstration of a precise relationship between the activation energy of proton conductivity and the number of adsorbed water molecules by using full-range data of a proton-conductive MOF. These results may provide a subtle but important refinement to the widely accepted empirical rule.

## Conclusions

In conclusion, Zr-BPT exhibited a wide range of proton conductivity and water vapor adsorption, depending on the partial pressure of water. It showed superprotic conductivity of  $3.6 \times 10^{-4} \text{ S cm}^{-1}$  at 25 °C under high humidity (0.98  $P/P_0$ ). The correlation between the structure, conductivity, and adsorption behavior revealed that the high proton conductivity is attributed to the presence of the Grotthuss mechanism, which is enabled by a large number of adsorbed water molecules. The relationship between activation energy and the number of adsorbed water molecules was clarified, indicating that the presence of the Grotthuss mechanism obviously decreases the activation energy. However, the commonly used criterion value for distinguishing the vehicle mechanism from the Grotthuss mechanism is somewhat ambiguous. These results provide important insights into the conduction mechanisms of proton-conducting MOFs.

## Conflicts of interest

There are no conflicts to declare.

## Data availability

All the data used are provided in the manuscript and the ESI.†

## Acknowledgements

The synchrotron radiation experiments were performed on the BL44B2 at SPring-8 with the approval of RIKEN (proposal no. 20220017).

## References

- 1 C. S. Gittleman, H. Jia, E. S. D. Castro, C. R. I. Chisholm and Y. S. Kim, Proton Conductors for Heavy-Duty Vehicle Fuel Cells, *Joule*, 2021, **5**, 1660–1677.
- 2 D.-W. Lim and H. Kitagawa, Rational Strategies for Proton-Conductive Metal–Organic Frameworks, *Chem. Soc. Rev.*, 2021, **50**, 6349–6368.
- 3 M. Sadakiyo, T. Yamada and H. Kitagawa, Hydrated Proton-Conductive Metal–Organic Frameworks, *ChemPlusChem*, 2016, **81**, 691–701.
- 4 S. Bureekaew, S. Horike, M. Higuchi, M. Mizuno, T. Kawamura, D. Tanaka, N. Yanai and S. Kitagawa, One-Dimensional Imidazole Aggregate in Aluminium Porous Coordination Polymers with High Proton Conductivity, *Nat. Mater.*, 2009, **8**, 831–836.
- 5 K. D. Kreuer, A. Rabenau and W. Weppner, Vehicle Mechanism, A New Model for the Interpretation of the Conductivity of Fast Proton Conductors, *Angew. Chem., Int. Ed. Engl.*, 1982, **21**, 208–209.
- 6 N. Agmon, The Grotthuss Mechanism, *Chem. Phys. Lett.*, 1995, **244**, 456–462.
- 7 K. D. Kreuer, S. J. Paddison, E. Spohr and M. Schuster, Transport in Proton Conductors for Fuel-Cell Applications: Simulations, Elementary Reactions, and Phenomenology, *Chem. Rev.*, 2004, **104**, 4637–4678.
- 8 S. Chand, S. C. Pal, D.-W. Lim, K. Otsubo, A. Pal, H. Kitagawa and M. C. Das, A 2D Mg(II)-MOF with High Density of Coordinated Waters as Sole Intrinsic Proton Sources for Ultrahigh Superprotic Conduction, *ACS Mater. Lett.*, 2020, **2**, 1343–1350.
- 9 M. Sadakiyo, T. Yamada, K. Honda, H. Matsui and H. Kitagawa, Control of Crystalline Proton-Conducting Pathways by Water-Induced Transformations of Hydrogen-Bonding Networks in a Metal–Organic Framework, *J. Am. Chem. Soc.*, 2014, **136**, 7701–7707.
- 10 P. Ramaswamy, N. E. Wong and G. K. H. Shimizu, MOFs as Proton Conductors – Challenges and Opportunities, *Chem. Soc. Rev.*, 2014, **43**, 5913–5932.
- 11 K. Shiraishi, K. Otsubo, K. Kato and M. Sadakiyo, A Novel Threefold Interpenetrated Zirconium Metal–Organic Framework Exhibiting Separation Ability for Strong Acids, *Chem. Sci.*, 2024, **15**, 1441–1448.
- 12 K. Zhang, R. P. Lively, C. Zhang, W. J. Koros and R. R. Chance, Investigating the Intrinsic Ethanol/Water Separation Capability of ZIF-8: An Adsorption and Diffusion Study, *J. Phys. Chem. C*, 2013, **117**, 7214–7225.
- 13 P. M. Schoenecker, C. G. Carson, H. Jasuja, C. J. J. Flemming and K. S. Walton, Effect of Water Adsorption on Retention of Structure and Surface Area of Metal–Organic Frameworks, *Ind. Eng. Chem. Res.*, 2012, **51**, 6513–6519.
- 14 Y. Yoshida, K. Kato and M. Sadakiyo, Vapor-Induced Superionic Conduction of Magnesium Ions in a Metal–Organic Framework, *J. Phys. Chem. C*, 2021, **125**, 21124–21130.
- 15 K. Otake, K. Otsubo, T. Komatsu, S. Dekura, J. M. Taylor, R. Ikeda, K. Sugimoto, A. Fujiwara, C.-P. Chou, A. W. Sakti, Y. Nishimura, H. Nakai and H. Kitagawa, Confined Water-Mediated High Proton Conduction in Hydrophobic Channel of a Synthetic Nanotube, *Nat. Commun.*, 2020, **11**, 843.
- 16 K. Kato, Y. Tanaka, M. Yamauchi, K. Ohara and T. Hatsui, A Statistical Approach to Correct X-ray Response Non-Uniformity in Microstrip Detectors for High-Accuracy and High-Resolution Total-Scattering Measurements, *J. Synchrotron Radiat.*, 2019, **26**, 762–773.



17 S. Kitagawa, R. Kitaura and S. Noro, Functional Porous Coordination Polymers, *Angew. Chem., Int. Ed.*, 2004, **43**, 2334–2375.

18 A. L. Spek, Single-Crystal Structure Validation with the Program PLATON, *J. Appl. Crystallogr.*, 2003, **36**, 7–13.

19 F. M. Richards, The Interpretation of Protein Structures: Total Volume, Group Volume Distributions and Packing Density, *J. Mol. Biol.*, 1974, **82**, 1–14.

20 BIOVIA, *Materials Studio 2020*, Dassault, San Diego, 2020.

21 I. Huskić, N. Novendra, D.-W. Lim, F. Topić, H. M. Titi, I. V. Pekov, S. V. Krivovichev, A. Navrotsky, H. Kitagawa and T. Friščić, Functionality in Metal–Organic Framework Minerals: Proton Conductivity, Stability and Potential for Polymorphism, *Chem. Sci.*, 2019, **10**, 4923–4929.

